IGNITION AND THERMAL STABILITY CHARACTERISTICS OF ADVANCED FUEL PLASMAS

J.H. Shultz, L. Bromberg and D.R. Cohn

Revised January 1980

Plasma Fusion Center Report RR-79-5

Ignition and Thermal Stability Characteristics of Advanced Fuel Plasmas[x]

J.H. Schultz[xx], L. Bromberg and D. R. Cohn

M.I.T. Plasma Fusion Center

Cambridge, Ma. 01239

[x] Supported by U.S. D.O.E. Contract EG-77-S-02-4183.A002

[xx] Westinghouse Corp.

Abstract

Ignition criteria and fusion power density are calculated for catalyzed-D and D-^{3}He plasmas for hot ion mode ($T_i > T_e$) operation facilitated by a large ratio of the ion energy confinement time to the electron energy confinement time. The optimistic case of complete transfer of the energy of the charged-particle fusion products to the ions is considered; this case further enhances hot ion mode operation. Even though hot ion mode operation increases the fusion power density, the maximum pressure-limited fusion power densities in catalyzed-D and D-^{3}He are at least a factor of thirty times lower than those in D-T plasmas; as a result the achievement of very high plasma beta and/or the maximum use of high field magnet technology are needed in order to attain high wall loadings and moderate thermal output power levels in D-D and D-^{3}He reactors. The implications of ignition requirements on machine design are determined for tokamak plasmas; the electron energy confinement time is assumed to be given by an empirical energy scaling law, $\tau_e \sim na^2$. The thermal stability of advanced fuel plasmas is studied. It is found that the runaway time is short compared to the energy confinement time for ion temperatures that maximize fusion power of a pressure limited plasma.

I. Introduction

Reactors which use advanced fusion fuels, such as catalyzed deuterium and D-^{3}He, are attractive because of the elimination of the need to breed tritium to produce their own fuel, reduced activation resulting from both reduced neutron load and increased choice of materials, reduced neutron damage and the possibility of highly efficient energy conversion cycles [1,2,3]. However, the ignition requirements are much more demanding and the fusion power densities are considerably lower than with D-T plasmas. Operation in the hot ion mode ($T_i > T_e$) has been suggested as a means to increase the energy multiplication factor Q and to reduce the ignition requirements with advanced fuels in the case where the energy balance is determined mainly by radiation [4,5]. It has also been shown that hot ion mode operation results in a significant reduction of the ignition requirements for D-T plasmas [4,6,7].

Control requirements for the burn of ignited advanced-fuel plasmas have not previously been considered. In time dependent codes [3,5,8], the plasma temperature is allowed to increase until the natural stable temperature is reached; operation at this temperature results in reduced fusion power for pressure-limited plasmas.

In this paper, electron thermal conduction losses are included in the study of hot ion mode operation of D-^{3}He and catalyzed deuterium plasmas, and thermal stability properties are calculated. As radiation plays a relatively small part in the energy balance, the dependence of the results on a model of synchroton radiation is reduced. The effect of hot ion mode operation on the fusion power density is calculated in section II. The possible reduction in ignition requirements and increase in fusion power density which could occur through complete energy transfer from the fast charged fusion products to the thermal ions is considered; this energy transfer might proceed through velocity space instabilities when $v_{fp} > v_A$, where v_{fp} is the speed of the fusion products and v_A is the Alfven speed [9]. In section III, an empirical scaling law for the electron energy confinement in tokamak plasmas [10] is used to calculate the ignition requirements in terms of the parameter $\beta a B^2$. In section IV, the thermal stability properties of advanced fuel plasmas are analyzed using a

multigroup description of the charged fusion products.

The results are compared with previous studies of advanced fuels and with a typical D-T reactor design.

II. Ignition criteria and Fusion Power Density

At ignition, the ion power balance is

$$0 = -\frac{1}{2}\frac{n_i T_i}{\tau_i} - \frac{3}{5}\frac{n_e (T_i - T_e)}{\tau_{ei}} + W_i \qquad (1)$$

and for the electrons

$$0 = -\frac{1}{2}\frac{n_e T_e}{\tau_e} + \frac{3}{5}\frac{n_e (T_i - T_e)}{\tau_{ei}} + W_e - P_{br} \qquad (2)$$

where n_e and n_i are the central electron and ion densities, T_e and T_i are the central electron and ion temperatures, τ_e and τ_i are the electron and ion energy confinement times, τ_{ei} is the electron-ion coupling time, and W_e and W_i are the electron and ion heating rates of the fast charged particles produced in the fusion reactions. W_i and W_e are calculated using the results of Sigmar and Joyce [11]. P_{br} represents the bremsstrahlung losses. Parabolic density and temperature profiles are assumed.

Synchrotron radiation has been neglected in (2). However, the effects of synchrotron radiation have been estimated by including the synchrotron losses from a tokamak plasma with $a \sim 1.5$ m and $B \sim 8$ T, using the results from [12]. In the temperature range considered in this paper, synchroton radiation is of the same order as bremsstrahlung radiation. The inclusion of synchrotron radiation lead to relatively minor changes in the results, as will be subsequently discussed.

Throughout this paper it is assumed that $\tau_i/\tau_e >> 1$ which maximizes hot ion mode operation. For $\tau_i/\tau_e >> 1$ the dominant ion energy loss mechanism is through ion-electron coupling. If the empirical scaling law for the electrons [10] and the neoclassical transport for the ions [13] hold at high temperatures in ignited advanced fuel tokamak plasmas, then $\tau_i/\tau_e >> 10$.

The dependence of the electron temperature at ignition upon ion temperature for $\tau_i/\tau_e >> 1$ is shown in Figure 1 for catalyzed-D and D-^{3}He plasmas. This figure is drawn for both classical slowing down of charged particle fusion products and for anomalous slowing down where all of the

energy of the charged fusion products goes directly into the ions [9]. The case of anomalous slowing down of the fusion products represents an optimistic lower bound on electron temperature at ignition.

Large temperature separations are not observed to occur at peak ion temperatures up to 150 keV for classical slowing down. With anomalous slowing, however, $T_i/T_e \sim 2.5$ at $T_i \sim 150$ keV for both D-^{3}He and catalyzed-D plasmas.

The values of $\overline{n_e \tau_e}$ required for ignition are shown in Figure 2 for catalyzed-D and for D-^{3}He. $\overline{n_e \tau_e}$ has a minimum at $T_i > 150$ keV of $(\overline{n_e \tau_e})_{min} \sim 2. \, 10^{20}$ m^{-3} s for both catalyzed-D and D-^{3}He. For comparison, for D-T, $(\overline{n_e \tau_e})_{min} \sim 3. \, 10^{19}$ m^{-3} s at $T_i \sim 50$ keV [7]. Including synchrotron radiation increases the value of $n \tau_e$ at ignition by < 40% for $50 < T_i < 150$ keV for both catalyzed-D and D-^{3}He for classical slowing down of the fusion products. The effects of including synchrotron radiation are smaller in the case of anomalous slowing down.

The fusion power density,

$$P_f \sim \sum_{species} r \, p_k \, p_l \, \langle \sigma \, v \rangle_{kl} \, E_{kl} \, \frac{\beta^2 \, B^4}{(T_i + T_e \, n_e/n_i + \overline{E_{fp} \, n_{fp}}/n_i)^2}$$

can be increased at a fixed T_i by increasing the ratio of T_i to T_e. Here p_k and p_l are the relative concentrations of species k and l, $\langle \sigma \, v \rangle_{kl}$ is the average fusion reactivity of the two species, and E_{kl} is the energy released in the fusion reactions. $\overline{E_{fp} \, n_{fp}}$ represents the contribution of the fast fusion products to the plasma pressure. B is the value of the magnetic field. β is the ratio of the average plasma pressure to the magnetic field pressure. $r = 1$ when $k \neq l$ and $r = 0.5$ when $k = l$.

The temperature dependence of the radially averaged pressure limited fusion power density, or specific fusion power density

$$\frac{P_f}{\beta^2 \, B^4}$$

is shown in Figure 3 for catalyzed-D and D-^{3}He. $P_f/\beta^2 B^4$ has relatively broad maxima for both fuel mixtures. The maximum values of $P_f/\beta^2 B^4$ are shown in Table I. The results for flat profiles are also shown for the purpose of comparison. Significant improvements in the power density of advanced reactors can be obtained by the inclusion of profile effects, as shown by Jassby and

Towner [14].

The results shown in Figures 1 and 3 are independent of the the electron energy balance equation (2). Therefore these results are independent of the assumptions concerning synchrotron radiation.

The maximum value of

$$\sum_{species} \frac{r\, p_k\, p_l\, \langle \sigma\, v \rangle_{kl}\, E_{kl}}{(T_i + T_e\, n_e/n_i + \overline{E_{fp}\, n_{fp}}/n_i)^2}$$

for advanced fuels is typically on the order of 100 times lower than the maximum value for D-T fuels. [2] However, the fusion power density of D-T reactor designs is often limited by neutron wall loading. As shown in Table II, reference advanced fuel reactor designs [15] have calculated fusion power densities up to one-tenth those of typical D-T reactor designs [16]. In contrast, the results in Table II show that for a plasma with $\beta \sim 10$ % and a toroidal field $B \sim 8$ T, a fusion power density of 2.3 MW/m^3, or about one third of that of present D-T reactor designs, would be achievable in D-^{3}He for parabolic profiles, under the optimistic assumption of anomalous slowing down of the charged fusion products.

III. Minimum $\beta\, a\, B^2$ for Ignition

The calculations in the previous section were independent of the particular scaling law of the electron energy confinement. In this section, we consider the consequences of using the empirical scaling law for the electron energy confinement [10],

$$\tau_e = 1.9\ 10^{-21}\ n_e\ a^2$$

where n_e is the peak electron density in m^3, a is the minor radius in m and τ_e is in s. If this scaling for the transport is assumed, the parameter $\beta\, a\, B^2$ scales as

$$\beta\, a\, B^2 \sim (n_e\, a)\,(T_e + T_i\,\frac{n_i}{n_e} + \frac{\overline{E_{fp}\, n_{fp}}}{n_e}) \sim (n_e\, \tau_e)^{1/2}\,(T_e + T_i\,\frac{n_i}{n_e} + \frac{\overline{E_{fp}\, n_{fp}}}{n_e}) \qquad (3)$$

Therefore, a criterion for ignition based on the product of macroscopic machine parameters, $\beta\, a\, B^2$ at ignition can be defined without reference to a specific machine design.

$(\beta\, a\, B^2)_{ign}$ is shown in Figure 4 for catalyzed-D and D-^{3}He as a function of the ion temperature. $(\beta\, a\, B^2)_{ign}$ has broad minima for both fuel mixtures considered. Table III gives the minimum value of $\beta\, a\, B^2$ required for ignition. Parabolic profiles result in a factor of two improvement in $(\beta\, a\, B^2)_{ign}$ for both fuel mixtures relative to the results for flat profiles. Anomalous slowing of the alpha particles further reduces the value of $(\beta\, a\, B^2)_{ign}$ by $\sim 20\,\%$ for catalyzed-D and by $\sim 40\,\%$ for D-^{3}He. If synchrotron radiation is included, the value of $(\beta\, a\, B^2)_{ign}$ for catalyzed-D and D-^{3}He increases by $< 20\%$ for $50 < T_i < 150$ keV for classical slowing down of the fusion products. Smaller increases in $(\beta\, a\, B^2)_{ign}$ due to synchrotron radiation occur in the case of anomalous slowing down.

The values of $\beta\, a\, B^2$ are shown in Table IV for the Illinois-Brookhaven advanced fuel reactor series [15]. The values of $\beta\, a\, B^2$ for these designs are about 10 times larger than those for a typical D-T reactor. In contrast, for a D-^{3}He reactor with parabolic profiles and anomalous slowing down, the calculated minimum value of $\beta\, a\, B^2$ is only three times that of the D-T reactor [16]. For example, with a field on axis of 8 T and a beta of 7 %, the minimum radius required for ignition in a D-^{3}He reactor would be equal to 1.5 m.

Based upon (3) the minimum thermal power level required for achieving ignition at a given wall loading P_w scales as

$$P_{th,\,ign} \sim P_w A\, a^2 \sim \frac{P_w A}{\beta^2 B^4} (n \tau_e)_{ign} \tag{4}$$

where A is the aspect ratio. Assuming that thermal equilibrium and stability control can be used to adjust the operating parameters (and therefore the power output), the characteristic thermal power output scales as

$$P_{th} \sim \frac{A P_w^3}{P_f^2} \sim \frac{A P_w^3}{\beta^4 B^8} \frac{(T_i + T_e n_e/n_i + \overline{E_{fp} n_{fp}}/n_i)^4}{(\langle \sigma v \rangle)^2} \tag{5}$$

It can be seen from both (4) and (5) that the high values of $(n \tau_e)_{ign}$ and the low values of P_f in advanced fuel reactors will result in very large thermal output power levels if wall loading levels similar to those in D-T reactor designs are desired. The use of high magnetic fields can have a very strong effect in reducing the thermal output power levels.

IV. Thermal Stability

In this section, the thermal stability of the plasma to temperature perturbations is studied. The methodology used in this study consists of linearizing the energy balance equations for the electron and for the ions, and solving for the eigenvalues of the system [7,17]. The growth rate is the real part of the eigenvalue with the largest real part and its inverse is defined as $\tau_{runaway}$. The fusion product dynamics are included by using a multigroup description for each of the fusion reaction products. The plasma density is assumed to remain constant during the perturbation. It is assumed that the electron energy confinement time τ_e is independent of the electron and ion temperatures (consistent with the empirical scaling law [10]) and that the ion energy confinement time is much larger than the electron energy confinement time. It is also assumed that the plasma does not expand against the confinining magnetic field (which results in a stabilizing force). [8,18]

Figure 5 shows the ratio $\tau_{runaway}/\tau_E$, where τ_E is the global energy confinement time,

$$\tau_E = \frac{T_e + T_i\, n_i/n_e}{T_e/\tau_e}$$

for D-^{3}He and for catalyzed-D as a function of the ion temperature. Figure 5 is drawn for classical slowing down of the charged fusion products; anomalous slowing down results in a factor of ~ 2 reduction of $\tau_{runaway}/\tau_E$. The runaway time can be significantly shorter than the energy confinement time, because of the large positive ion temperature dependence of the fusion reactivity. Ion temperatures larger than 150 keV are required for stability.

Synchrotron radiation has not been included in these calculations. The main effect of including this radiation is to lower the necessary ion temperature for stability to the range 130-150 keV.

Operation at a stable point significantly decreases the achievable specific fusion power $P_f/\beta^2\, B^4$, increases the requirements on $\beta\, a\, B^2$, and involves a very large extrapolation from experimentally observed plasmas. The requirements needed for temperature control at the lower unstable equilibrium temperature have to be compared with the disadvantages of operating at the

higher stable temperature.

V. Conclusion

The effects due to a large ratio of the ion energy confinement time to the electron energy confinement time have been studied for catalyzed-D and D-^{3}He fuels. The following results have emerged.

If anomalous transfer of charged particle fusion product energy to the ions occurs, the fusion power density can be increased by about a factor of two and the minor radius can be reduced by about a factor of two for D-^{3}He. The beneficial effects on catalyzed-D are somewhat smaller.

The intrinsic thermal stability of D-^{3}He and catalyzed-D advanced fuel reactors, expressed as the ratio of thermal runaway time to the energy confinement time, appears to be less than that of a D-T reactor. Very high temperatures (T_i > 120 keV) are required for intrinsic thermal stability.

Under the conditions where $\tau_i/\tau_e >> 1$ and where there is anomalous tranfer of charged particle fusion products to the ions, a D-^{3}He tokamak reactor with $\beta \sim 10\%$ and a magnetic field of 8 T and parabolic density and temperature profiles would have a fusion power density of about one third of that of present D-T reactor designs.

Either the achievement of very high plasma beta and/or the maximum use of high field magnet technology is needed in order to develop D-D and D-^{3}He reactor designs with high wall loadings and moderate thermal output levels.

Acknowledgements

The authors wish to thank Dr. J.L. Fisher for useful discussions.

References

1 See, for example, MILLS, R.G., in *Proceedings of the Fourth Symposium on the Engineering Problems of Fusion Research*, IEEE Trans Nuc Sci NS-18 (1974)

2 MILEY, G.H., *Fusion Energy Conversion*, Am. Nucl. Soc (1976)

3 McNALLY, J.R., Jr, Nucl Fusion 18 (1978) 133

4 CORDEY, J.G., in *Proceedings of the Fourth Symposium on Plasma Heating in Toroidal Devices*, Varenna, Italy (1977)

5 McNALLY, J.R., Jr, in *Proceedings of the Sixth IEEE Symposium on Engineering Problems of Fusion Research*, San Diego, Calif. (1976), 1012

6 CLARKE, J.F., U.S. Department of Energy; submitted for publication to Nucl. Fusion

7 BROMBERG, L., COHN, D.R. and FISHER, J., Nucl Fusion 19 (1979) 1359

8 POWELL, C. and HAHN, O., Nucl Fusion 12 (1972) 663

9 MOLVIG, K. and SIGMAR, D.J., M.I.T. Plasma Fusion Center, private communication (Jan 1979); manuscript in preparation

10 COHN, D.R., PARKER, R.R. and JASSBY, D.L., Nucl Fusion 16 (1976) 31; JASSBY, D.L., COHN, D.R. and PARKER, R.R., Nucl Fusion 16 (1976) 1045

11 SIGMAR, D.J. and JOYCE, G., Nucl Fusion 11 (1971) 447

12 KRAJCIK, R.A., Nucl Fusion 13 (1973) 7

13 HINTON, F.L. and HAZELTINE, R.D., Rev of Modern Phys. 48 (1976) 239

14 JASSBY, D.L. and TOWNER, H.H., Princeton Plasma Physics Laboratory Report PPPL-1360 (June 1977)

15 CHOI, C.K., GERDIN, G.A., MILEY, G.H. and SOUTHWORTH, F.H., Exploratory Studies of High Efficiency Advanced Fuels Fusion Reactors, EPRI Annual Report ER-581 (Nov 1977)

16 COHN, D.R. *et al.*, MIT Plasma Fusion Center Report RR-79-2 (Jan 1979)

17 See, for example: YAMATO, H., M. OHTA and S. MORI, Nucl Fusion 12 (1972) 604; MADDEN, P.A. (et al.), Fusion Reactor Control Study, Second Annual Report, C.S. Draper Lab Report R-1268 (1978)

18 LACKNER, K. and WILHELM, R., Max Planck Institut fur Plasma Physik, Garching, Germany, private communication

List of Figures

TABLE I

Average Power Density and Average Specific Power Density for Advanced Fuel Plasmas

Fuel	Slowing	Profile	$\langle T_i \rangle$ (keV) at $P_{f,\,max}$	$P_{f,\,max}/\beta^2 B^4$ ($MW/m^3 T^4$)	P_f (MW/m^3) for $\beta = 0.1$, $B = 8.0$ T
Cat-D	Classical	Flat	38	.019	0.78
D-^{3}He	Classical	Flat	70	.021	0.86
Cat-D	Anomalous	Flat	48	.024	0.96
D-^{3}He	Anomalous	Flat	80	.034	1.40
Cat-D	Classical	Parabolic	21	.033	1.35
D-^{3}He	Classical	Parabolic	41	.035	1.43
Cat-D	Anomalous	Parabolic	29	.038	1.56
D-^{3}He	Anomalous	Parabolic	49	.055	2.25

TABLE II

Averaged Specific Power Density and Averaged Power Density for Reference Tokamak Reactors

Reactor	Fuel	T_i(keV)	P_f (MW/m^3)	P_f/β^2B^4 ($MW/m^3 - T^4$)
ILB-CHβ[a]	Cat-D	45	.72	.016
ILB-CLβ[a]	Cat-D	45	.83	.016
ILB-DHβ[a]	D-^{3}He	45	.83	.016
ILB-DLβ[a]	D-^{3}He	45	.57	.016
HFCTR[b]	D-T	12	7.7	1.60

[a] From reference [15]

[b] From reference [16]

TABLE III

Minimum βaB^2 for Ignition for Advanced Fuel Plasmas

Fuel	Profile	Slowing	$\langle T_i \rangle$ (keV) at $(\beta aB^2)_{min}$	$(\beta aB^2)_{min}$ (mT^2)
Cat-D	Flat	Classical	43	25
D-^{3}He	Flat	Classical	72	23
Cat-D	Flat	Anomalous	50	19
D-^{3}He	Flat	Anomalous	87	13
Cat-D	Parabolic	Classical	28	13
D-^{3}He	Parabolic	Classical	40	12
Cat-D	Parabolic	Anomalous	30	11
D-^{3}He	Parabolic	Anomalous	48	7

Table IV

βaB^2 for Ignited Reference Tokamak Reactors

Reactor	Fuel	R(m)	β_T	a(m)	$B_T^2(T^2)$	βaB^2 (mT^2)
ILB-CHβ [a]	Cat-D	10.6	0.3	3.5	22.1	23.2
ILB-CLβ [a]	Cat-D	13.2	0.12	4.4	59.3	31.3
ILB-HHβ [a]	D-^{3}He	7.6	0.3	2.53	30.3	23.0
ILB-HLβ [a]	D-^{3}He	8.3	0.12	2.75	49.0	16.2
HFCTR [b]	D-T	6.0	0.04	1.2	54.8	2.63

[a] From reference [15]

[b] From reference [16]

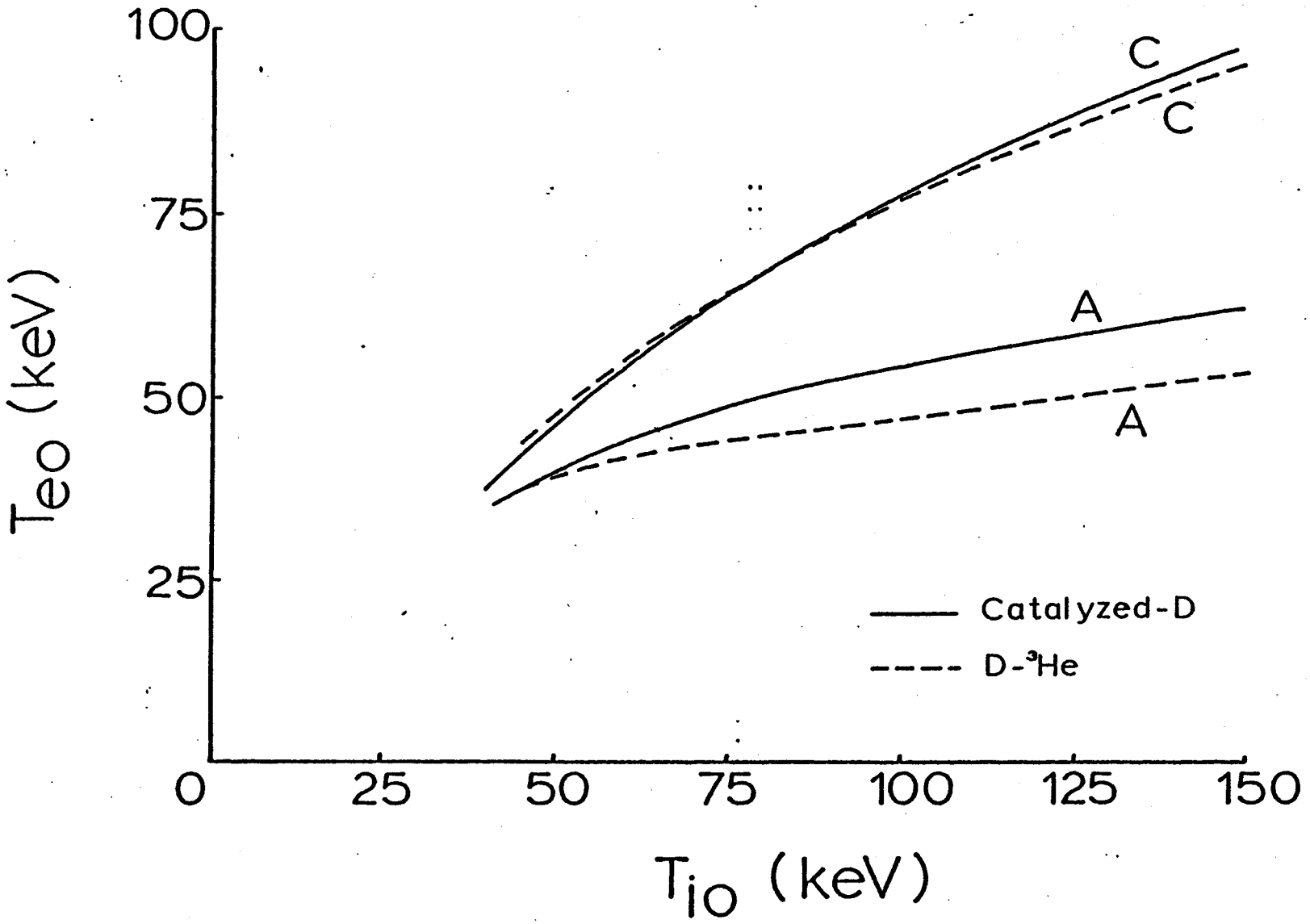
100
75
50
25
0
25
50
75
100
125
150
T_{eo} (keV)
T_{io} (keV)
C
C
A
A
Catalyzed-D
D-^{3}He

Figure 1

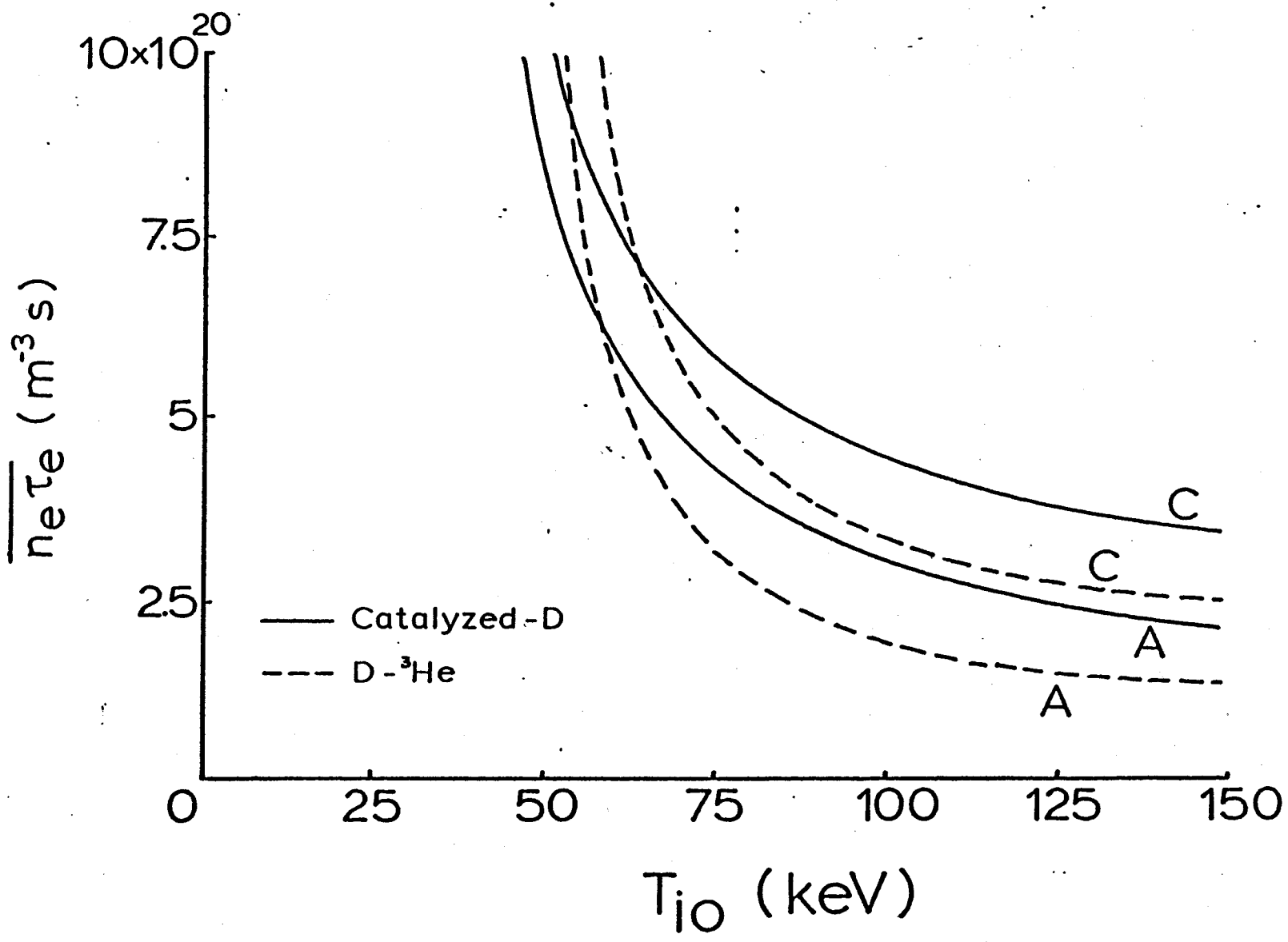
10×10^20
7.5
5
2.5
0
25
50
75
100
125
150
$\overline{n_e \tau_e}$ (m^{-3} s)
T_{io} (keV)
Catalyzed-D
D-^{3}He
C
C
A
A

Figure 2

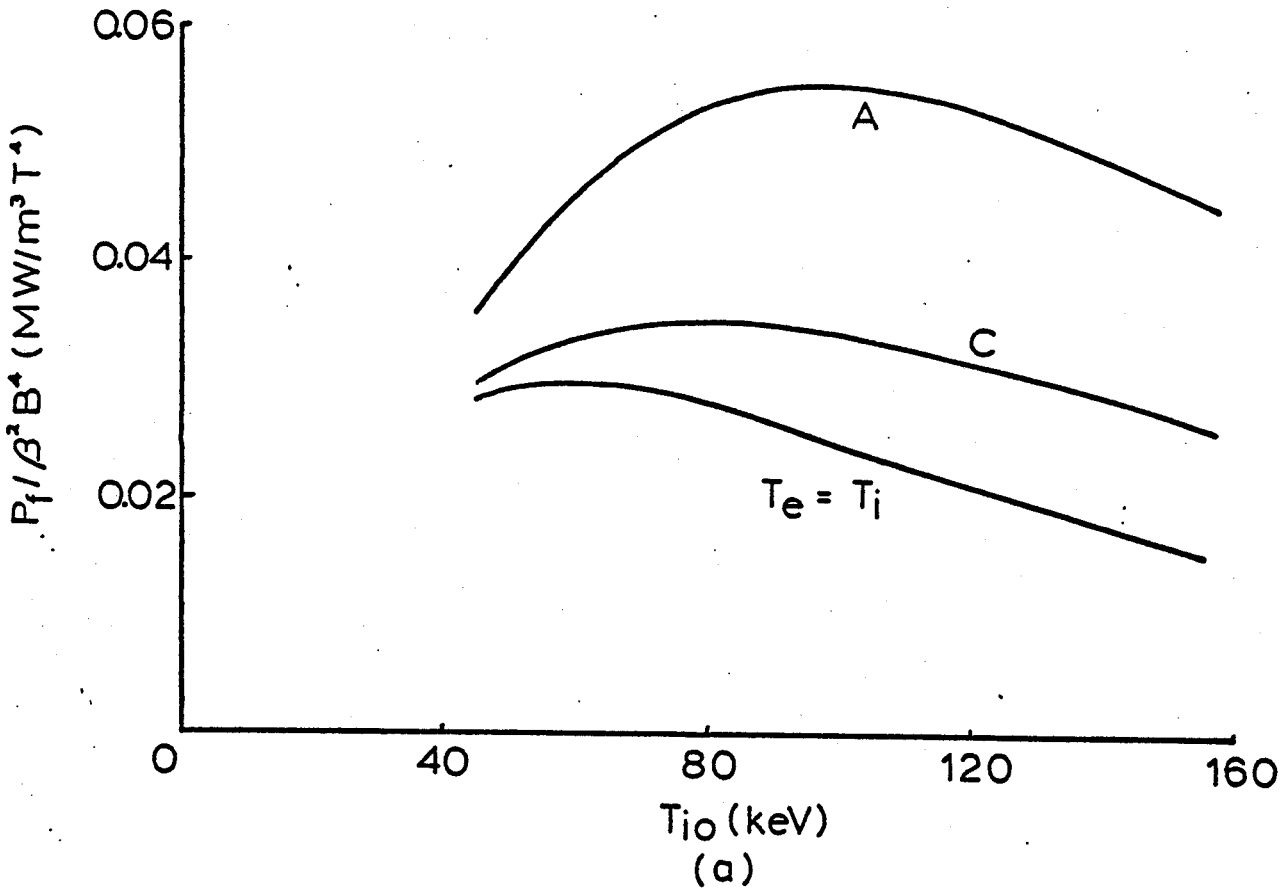
0.06
0.04
0.02
0
40
80
120
160
A
C
$T_e = T_i$
$P_f/\beta^3 B^4$ (MW/m^{3}T^4)
T_{io} (keV)
(a)

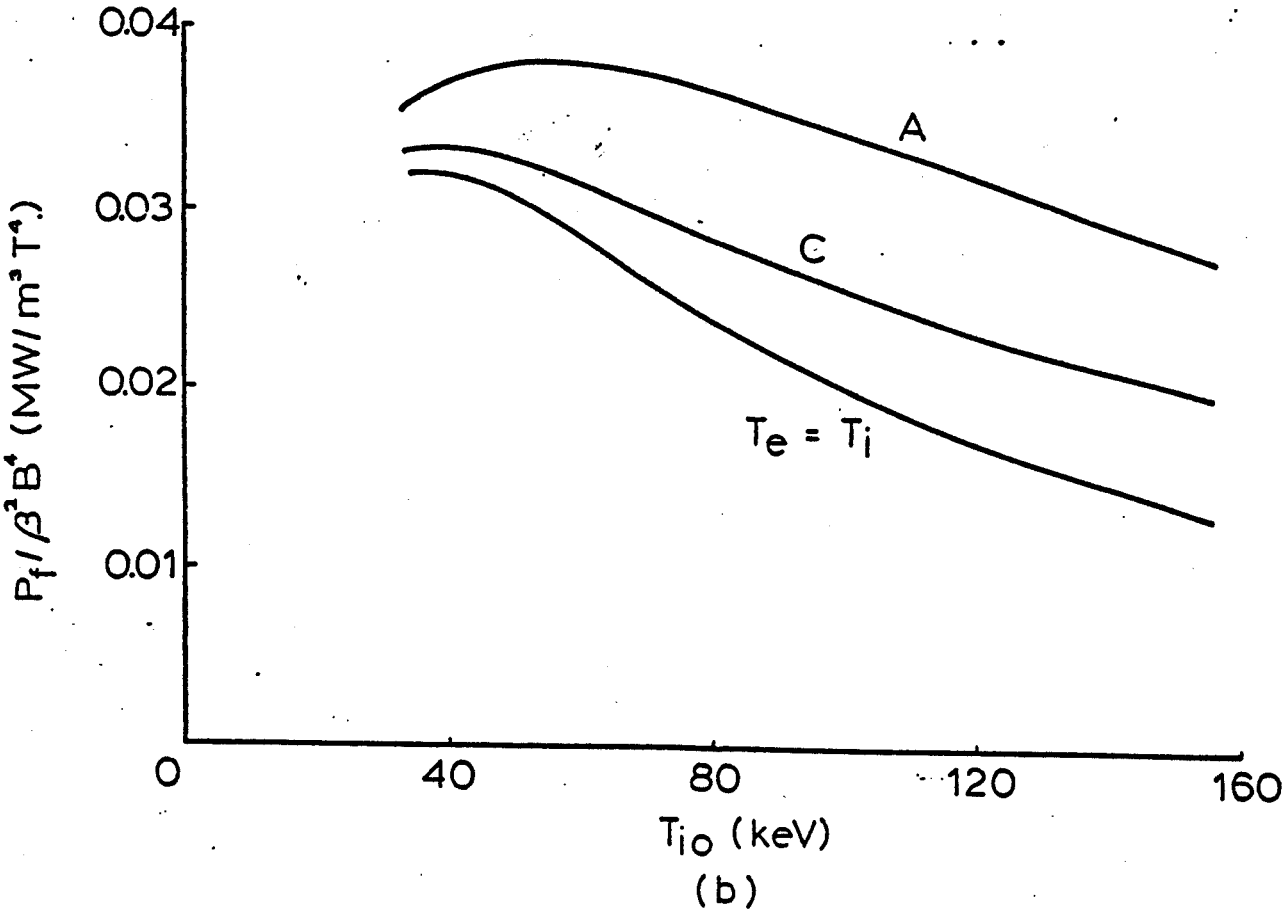
0.04
0.03
0.02
0.01
0
40
80
120
160
A
C
$T_e = T_i$
$P_f/\beta^3 B^4$ (MW/m^{3}T^4)
T_{io} (keV)
(b)

Figure 3

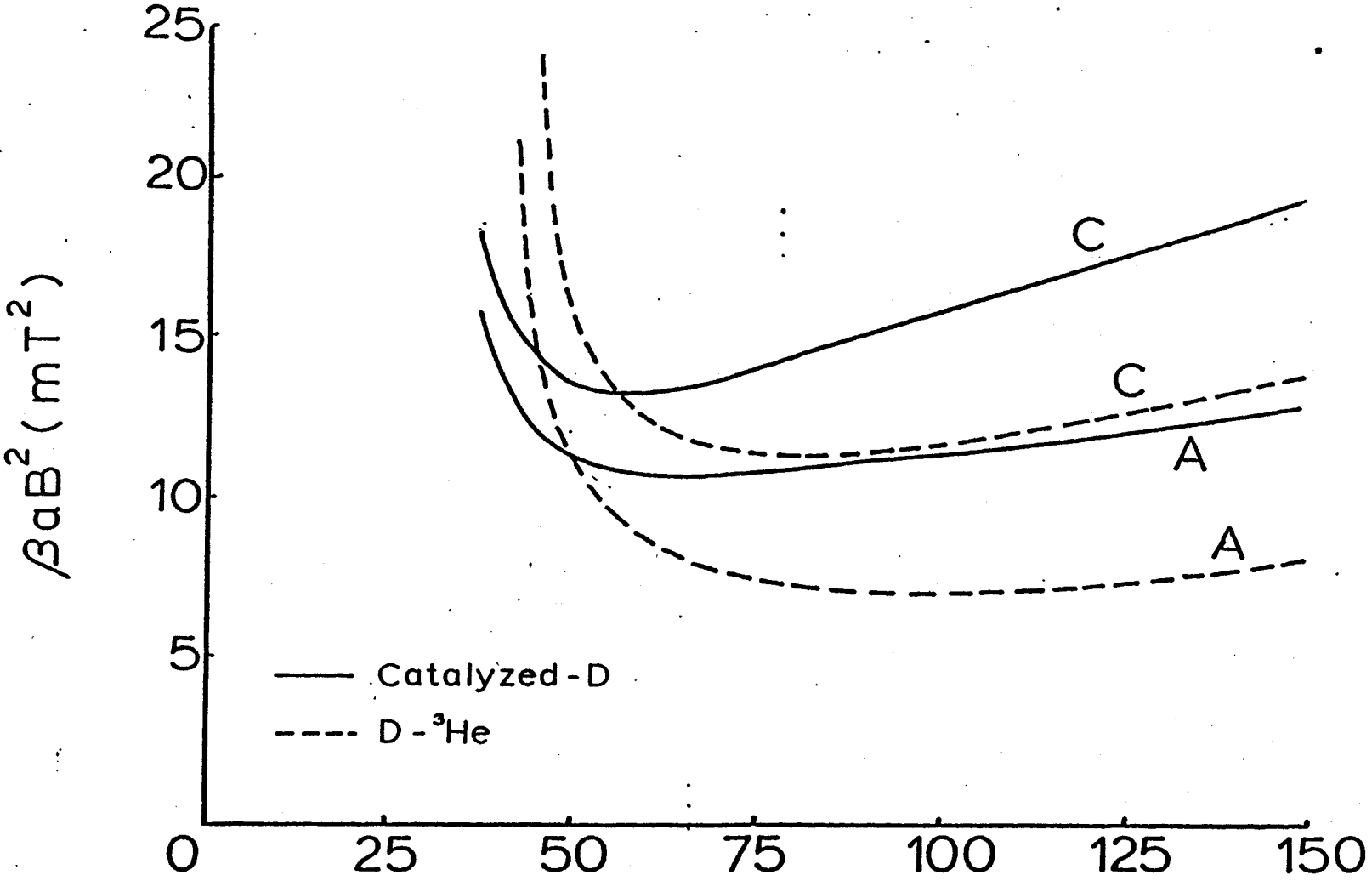
25
20
15
10
5
0
25
50
75
100
125
150
$\beta aB^2 (mT^2)$
T_{io} (keV)
C
C
A
A
Catalyzed-D
D-^{3}He

Figure 4

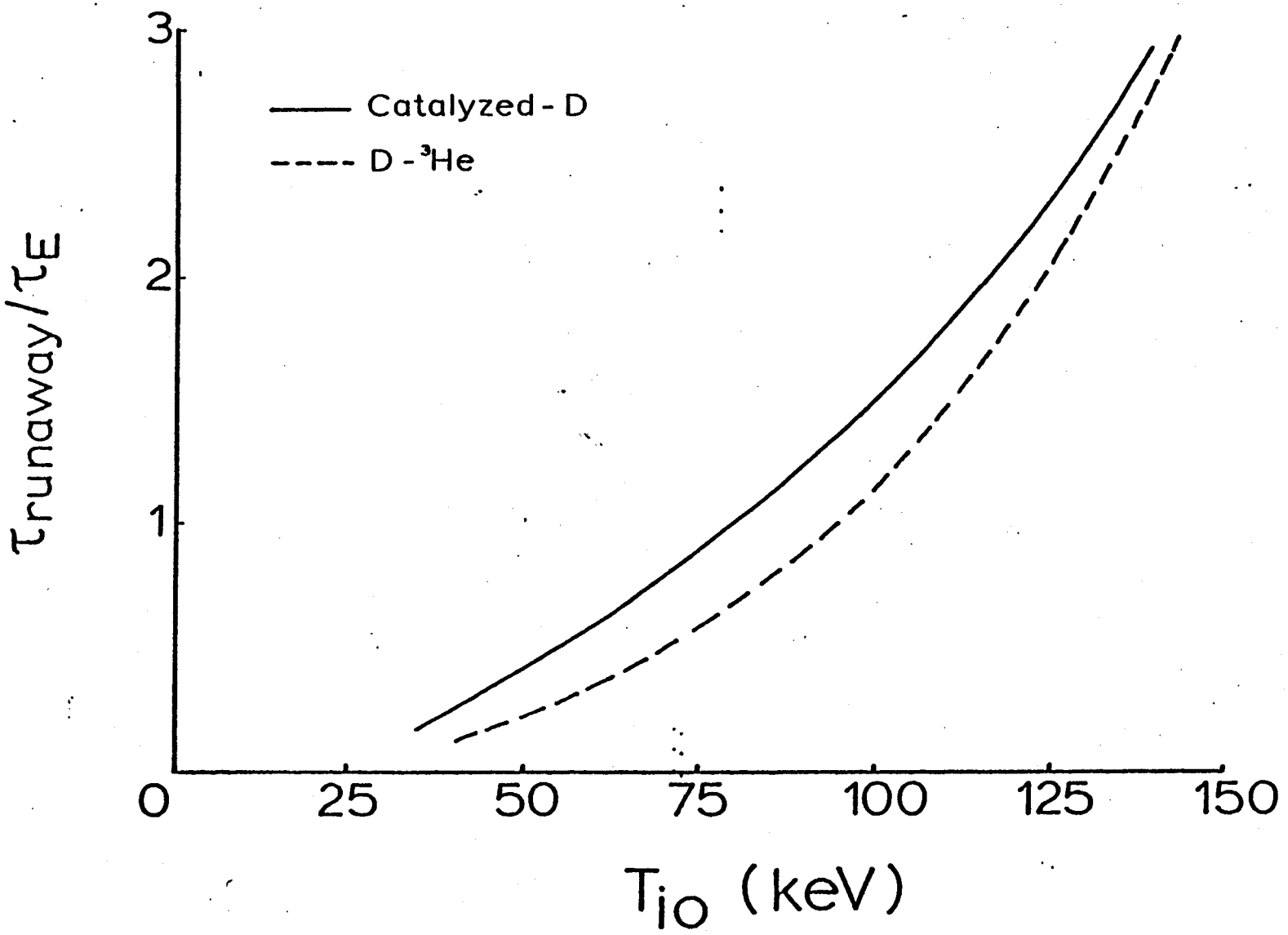

Figure 5